Contents lists available at ScienceDirect

Materials and Design

journal homepage: www.elsevier.com/locate/matdes



Oxidation–nitridation-induced recrystallization in a near- α titanium alloy



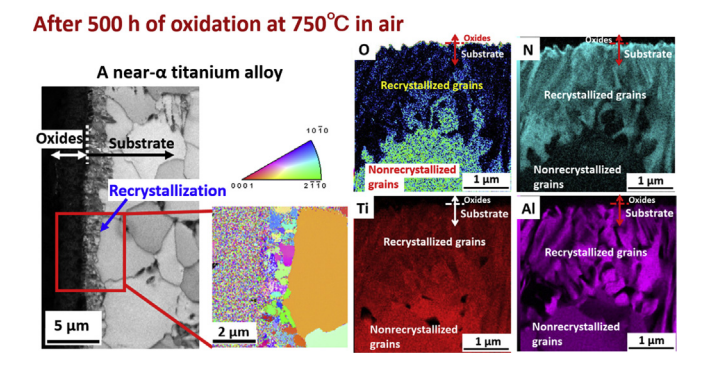
Tomonori Kitashima ^{a,b,*}, Toru Hara ^a, Yang Yang ^{a,b}, Yuka Hara ^a

- ^a National Institute for Materials Science, 1-2-1 Sengen, Tsukuba, Ibaraki 305-0047, Japan
- ^b Kyushu University; 744 Motooka Nishi-ku, Fukuoka 819-0395, Japan

HIGHLIGHTS

- Recrystallization at the oxide-metal interface in a titanium alloy was caused by the formation of nitrides during oxidation.
- Before the recrystallization at the interface, nitrogen dissolved in the substrate, and a nitrogen-rich layer formed near the interface.
- The oxygen concentration was lower in the recrystallized grains compared with that in the nonrecrystallized grains.

GRAPHICAL ABSTRACT



$A\ R\ T\ I\ C\ L\ E \qquad I\ N\ F\ O$

Article history: Received 6 July 2017 Received in revised form 12 October 2017 Accepted 14 October 2017 Available online 16 October 2017

Keywords: Oxidation Ti alloy Recrystallization Nitrogen

ABSTRACT

The oxidation resistance of titanium alloys is an important property for high-temperature applications. Here, the oxidation–nitridation-induced recrystallization at the oxide–metal interface of a near- α titanium alloy substrate was analyzed using electron–backscatter diffraction and scanning transmission electron microscopy after oxidation tests at 750 °C for 500 h in air. Oxidation–nitridation-induced recrystallization was promoted by the enrichment of nitrogen at the interface, and grains comprising Ti_2N and Ti_3AlN grew from the interface with the inhomogeneous distribution of nitrogen.

© 2017 Elsevier Ltd. All rights reserved.

1. Introduction

Near- α titanium alloys have been used for fabricating the compressor components of jet engines. Oxidation resistance is an important property required for materials used in high-temperature applications (for example, see [1]). During oxidation of near- α titanium alloys, Al₂O₃ and TiO₂ form and grow on the metal surface and an oxygenrich zone, called the " α -case," forms in the substrate near the surface

E-mail address: KITASHIMA.Tomonori@nims.go.jp (T. Kitashima).

because of the dissolution of oxygen [2,3]. The growth of those oxides and α -case causes surface and sub-surface embrittlement. Therefore, to avoid the degradation of mechanical properties as a result of the oxidation of near- α titanium alloys, limiting the growth of oxides formed on their surface and the growth of the α -case is important.

The oxidation behavior of $\alpha+\beta$ titanium alloys has been previously studied [4]. During the oxidation of Ti-6Al-4 V and near- α titanium alloys, internal TiO₂ and external Al₂O₃ layers are formed on the surface, and these oxides form an alternate multilayer after long exposure at high temperatures [5–7,9]. Although the oxidation kinetics of $\alpha+\beta$ titanium alloys is essentially governed by TiO₂ formation [10], the oxidation behavior is strongly affected by alloying elements in titanium

^{*} Corresponding author at: National Institute for Materials Science, 1-2-1 Sengen, Tsukuba, Ibaraki 305-0047, Japan.

alloys. Kitashima et al. demonstrated the role of each alloying element in the oxidation behavior and the beneficial effect of added aluminum, silicon, zirconium, and niobium in improving oxidation resistance [11]. Recently, the effect of the addition of gallium, an α -stabilizing element, on the oxidation behavior of titanium alloys was studied. The addition of gallium stabilized the formation of an Al_2O_3 layer because of the dissolution of Ga_2O_3 in Al_2O_3 [9]. In a previous study, we found that recrystallization occurred in the substrate of a gallium-added alloy near the oxide/metal interface; notably, the addition of tin instead of gallium did not induce similar recrystallization [12].

The literature contains few reports of such recrystallization during oxidation. Liu et al. investigated recrystallization at the oxide/metal interface during oxidation in a binary Ni-Cu alloy; they referred to this phenomenon as oxidation-induced recrystallization and suggested that one of the reasons for the recrystallization was the stress generated at the oxide/metal interface as a result of volume change [13]. In addition, the recrystallization may be partly induced by the lattice Kirkendall effect generated by the fast diffusion of nickel toward the oxide/metal interface under the driving force of preferential nickel oxidation at higher temperatures [13]. In a previous study, we observed recrystallization at the oxide/metal interface in a multicomponent near- α titanium alloy upon the addition of gallium as an α -stabilizing element [12]. The mechanism of the recrystallization process in titanium alloys remains unclear. Oxygen and nitrogen, which penetrate from the metal surface, are also α -stabilizing elements and tend to be abundant on the metal surface of the titanium alloy during oxidation. In this study, we analyzed the recrystallization of a near- α titanium alloy during oxidation, focusing on the diffusion of α -stabilizing elements. We used a scanning transmission electron microscope equipped with windowless double detectors with a large detecting area (100 mm²) to improve the detecting efficiency, particularly for light elements.

2. Experimental procedure

An ingot (1.1 kg) of a near- α titanium alloy TKT 41 was produced using the cold crucible levitation melting method. The chemical composition of the TKT 41 alloy is 7.0 Al, 3.0 Ga, 6.0 Zr, 1.0 Mo, 1.0 Nb, 0.2 Si (in wt%), with balance Ti. The concentration of oxygen was measured by the inert gas fusion infrared absorption method; the oxygen concentration was 0.093 wt%. The aluminum equivalence of this alloy, calculated by Al + $1/2 \times Ga + 1/3 \times Sn + 1/6 \times Zr + 10 \times O$ in wt% [14,15], was equal to 10.4. The alloy was melted twice to enhance its compositional uniformity. The β-transus temperature, which was measured by microstructural observation, was 995 °C \pm 5 °C. The cast ingot was β -forged at 1130 °C and then groove-rolled to 90% reduction at 980 °C in the $\alpha + \beta$ temperature region to form square rods with 14-mm sides. The rods were further annealed at 970 °C in the $\alpha + \beta$ temperature region for 1 h, followed by air cooling. The rod was subsequently aged at 700 °C for 2 h and then air cooled. Cylindrical specimens (8 mm in diameter and 4 mm in height) were machined from the heat-treated bars for the oxidation tests.

The surfaces of the specimens were polished using #800-grit SiC paper, followed by ultrasonic cleaning in acetone. After sample preparation, an isothermal oxidation test was performed in air at 750 °C. The samples in alumina crucibles placed in the furnace during oxidation were removed from the furnace after 20, 45, 70, 90, 110, 140, 240, 340, and 500 h of the oxidation test. The analysis of the weight gain of this alloy during oxidation has been reported elsewhere [12]. After oxidation testing, the oxidized samples were cold mounted, cut, and metallographically polished finally using (i) a 3-µm polycrystalline diamond suspension and a Buehler TriDent pad and (ii) a colloidal silica suspension (0.06 µm) and a Buehler ChemoMet pad. The samples were subsequently cleaned by argon-ion milling using a Fischione Instruments Model 1060 SEM Mill. The cross-sectional microstructures of the oxidized samples were analyzed via scanning electron microscopy (SEM, ZEISS Auriga) and electron-backscatter diffraction (EBSD) observations

(performed with the EBSD module attached to the SEM equipment) at an accelerating voltage of 15 kV using an AMETEK DigiView 5 detector. Chemical analyses were performed by energy-dispersive X-ray spectroscopy (EDS) using a spectrometer attached to the scanning electron microscope; EDS was performed at an accelerating voltage of 15 kV using an Ametek Octane Super 60 mm² detector. A scanning transmission electron microscope (STEM, JEOL JEM-2800) equipped with double energy-dispersive X-ray spectroscopy (EDS) detectors was also used. Each detector in this scanning transmission electron microscope has a large detecting area (100 mm²) and is windowless to improve its detection efficiency, particularly for light elements. The following spectral lines were chosen for each element in the EDS analysis: N:K; O:K; Al:K; Si:K; Ti:K; Ga:K; Zr:L; Nb:L; and Mo:L. EDS elemental concentration profiles were obtained along an approximately 100-nm-wide line. Scanning transmission electron microscopy (STEM) samples were prepared using the focused ion beam (FIB, Zeiss Auriga) milling technique. The sample surface was protected by depositing platinum before gallium FIB milling. After the sample was sliced and lifted, it was affixed to a transmission electron microscopy (TEM) mesh. The sample was thinned from both sides to a final thickness of less than 100 nm. The final beam current used was 20 pA with an accelerating voltage of 5 kV.

The oxidized samples after 20 h and 500 h of the oxidation test were prepared for TEM using a twin-jet electropolisher. An electrolyte mixture of 10% perchloric acid, 30% n-butyl alcohol, and 60% methanol was used to prepare the electron-transparent regions from -40 to $-30\,^{\circ}\text{C}$ at 20 V. To confirm the precipitation of the α_2 phase in the substrates, the oxidized samples were observed using a JEOL-2100 transmission electron microscope operated at an accelerating voltage of 200 kV.

3. Results and discussion

The microstructure of the as-heat-treated bar, which is shown in Fig. 3(c) in Ref. 8, comprised a bimodal microstructure with primary α and lamellar structures. The weight gain of a sample per unit area for TKT 41 is shown in Table 1. The microstructures after 20 h and 500 h of the oxidation test are shown in Fig. 1(a) and (e). Both the samples exhibit a bimodal microstructure with primary α and lamellar structure, wherein the dark and bright phases are the α phase with a hcp structure and the β phase with a bcc structure, respectively. However, the β phase coarsened and its volume fraction was smaller than that of the as-heattreated microstructure. The Al equivalence of the current alloy is 10.4, which is sufficiently high for the α_2 phase of the D0₁₉ structure to precipitate in the bulk. The precipitation of the α_2 phase in the bulk of both samples was observed, as shown in dark-field images and diffraction patterns in Fig. 1(b) and (f). Both samples contained an unknown phase mainly on grain boundaries; examples are shown as circles in Fig. 1(e). The color of the unknown phase on the backscattered-electron image is similar to the β phase. This phase contained high concentrations of Ga and Mo; however, it could not be identified in this study because its small size precluded analysis by EDS.

The recrystallization at the oxide/metal interface was not clearly observed after 20 h of oxidation, as shown in Fig. 1(c) and (d). However, as the oxidation time was increased to 500 h, the thickness of the oxide layers increased and recrystallized fine grains in the substrate near the oxide/metal interface grew. The image quality (IQ) map in Fig. 1(g) shows clear boundaries between the oxide and the recrystallized zone in the substrate and between the recrystallized and the nonrecrystallized zones in the substrate. The large grain size in the

Table 1Measured weight gain of TKT 41 oxidized at 750 °C for times ranging from 0 to 500 h.

Time (h)	0	20	45	70	90	110	140	240	340	500
Weight gain (mg/cm²)	0.0	0.56	0.74	0.87	1.05	1.18	1.24	1.42	1.73	1.92

Download English Version:

https://daneshyari.com/en/article/7217644

Download Persian Version:

https://daneshyari.com/article/7217644

<u>Daneshyari.com</u>